Plosila, P., Vierelä, R., Juntunen, P., Kesti, V., Kömi, J. & Kaijalainen, A. (2025). An investigation on behaviour of 800 MPa grade hot-rolled steels in interrupted ISO 16630 hole expansion testing. MATEC Web of Conferences, 408, 01073

DOI: https://doi.org/10.1051/matecconf/202540801073

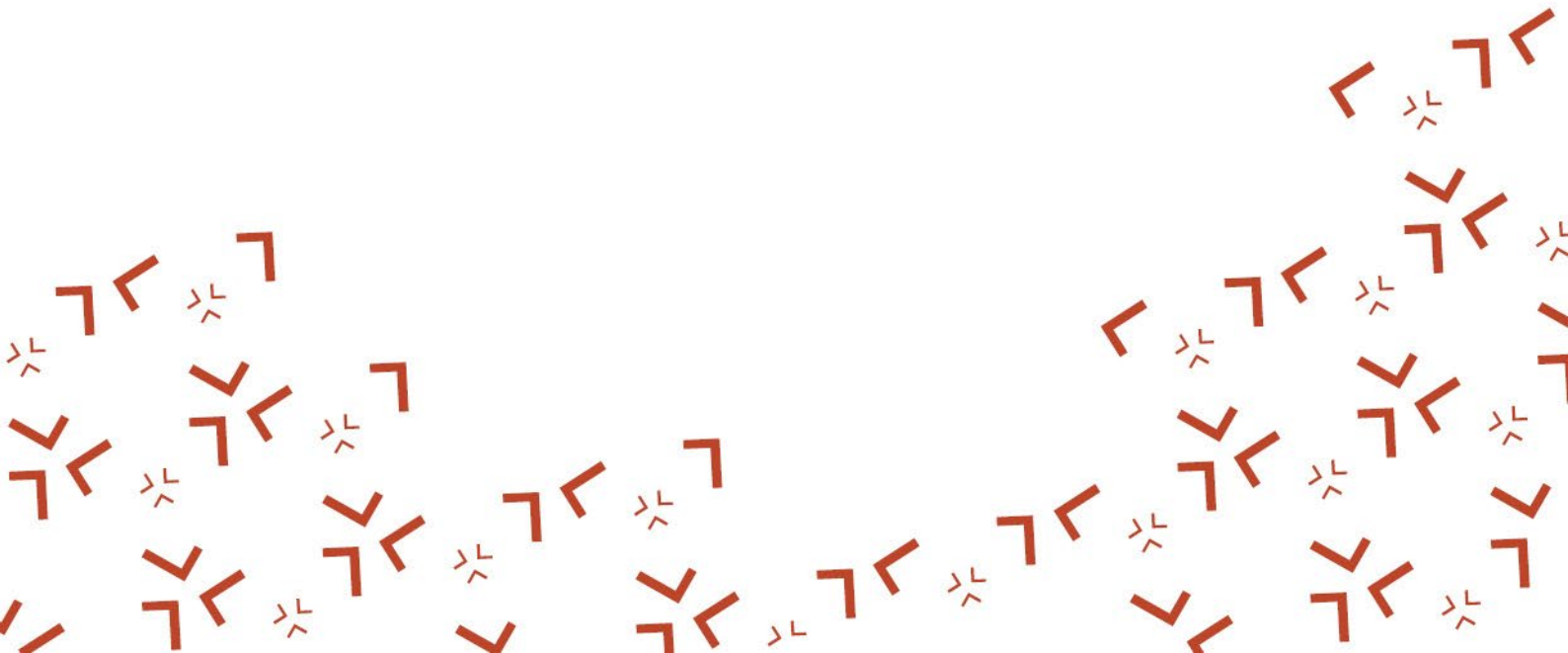

An investigation on behaviour of 800 MPa grade hot-rolled steels in interrupted ISO 16630 hole expansion testing

Pekka Plosila[1*], *Raimo* Vierelä[2], *Päivi* Juntunen[2], *Vili* Kesti[3], *Jukka* Kömi[1], and *Antti* Kaijalainen[1]

[1]University of Oulu, Materials and Mechanical Engineering, 90570 Oulu, Finland
[2]Lapland University of Applied Sciences, New Industry, 94600 Kemi, Finland
[3]SSAB Europe, Knowledge Service Center, 92100 Raahe, Finland

Abstract. The ISO 16630 hole expansion test is the most widely used method for investigating the stretch-flangeability of steels. However, the limiting hole expansion ratio (HER) does not provide detailed information on the behaviour of the edge during the expansion process. Digital image correlation (DIC) strain measurements allow a more detailed analysis of formability testing. In the standard hole expansion test, accurate imaging of the surface close to the edge is challenging. The aim of this study was to investigate the cut-edge behaviour of high-strength hot-rolled steels with similar tensile strengths at various points in the hole expansion test. Interrupted ISO 16630 tests with punched holes were conducted by discontinuing the tests at different punch strokes. Instead of DIC strain measurement, the specimens were 3D scanned after testing to investigate the thinning of the edge in different sheet directions. Additional tests were performed on specimens with wire electrical discharge machined (W-EDM) holes for comparison. The results showed considerable localisation of edge thinning in the W-EDM specimens, however some localisation was also observed in the punched specimens prior to failure. The deformation along the hole edge is more uniform in the material with the least planar anisotropy.

Keywords: High-strength steel; Stretch-flangeability; Edge cracking; Anisotropy.

1 Introduction

Hot-rolled advanced high-strength steels have seen increasing interest in the automotive and transportation industry for their potential for weight reduction, cost-effectiveness, and good mechanical properties. The potential applications of these steels include chassis and suspension parts. Due to requirements for efficiency and high production volumes, manufacturing of components often involve blanking followed by cold forming operations. Mechanical cutting process during blanking introduces highly localised deformation and damage to the material, which limits the formability of the sheared edges [1].

The ISO 16630 hole expansion test (HET) [2] is a standardised method for evaluating the suitability of sheet metals for forming processes involving stretch-flanging. In the test, a 10 mm diameter punched hole is expanded with a conical tool until a through-thickness crack is observed. Although the ISO 16630 HET is widely used to evaluate susceptibility of materials to edge cracking, the test has limitations, such as high amount of scatter in results [3] and major dependence on the testing conditions [4, 5]. Additionally, the result of the test, the limiting hole expansion ratio (HER), as a single-value metric does not provide a detailed description on the behaviour of the edge during the forming process, which can have significant differences between different materials.

Today, digital image correlation (DIC) is widely used for local strain measurement during different formability tests. For the ISO 16630 HET, however, the DIC strain measurement is challenging due to the conical expansion tool geometry. As the advancing expansion tool starts to form the flange, the initially vertical hole surface will start to approach horizontal level, which can make observation of the sheet surface close to the hole edge difficult. Additionally, as the flange and the expansion tool are moving towards the cameras, the view to the sheet surface can be blocked from the opposite side camera, especially with high hole expansion ratios.

Alternative test set-up geometries can make the DIC strain measurement feasible during hole expansion. Results showing localisation of circumferential strain in different sheet directions during hole expansion testing of high-strength hot-rolled steels with hemispherical and flat-top expansion tool have been reported [6, 7]. However, the alternative test set-up geometries produce different strain gradients in the edge [8]. Materials can have different responses to these strain gradients and localisation of deformation [5, 9], thus the measurement results with the alternative tool geometries may not always be indicative of the hole expansion performance with the standard conical tool set-up.

3D scanning is a possible option for investigating localisation of deformation in hole expansion test

* Corresponding author: pekka.plosila@oulu.fi

specimens. By capturing surface topography on both sides of the specimen, thickness in various locations can be measured, and by comparing the measured thickness to the initial thickness of the sheet, (plastic) thinning near the hole edge can be determined.

The aim of this study was to investigate behaviour of advanced high-strength hot-rolled steels with similar tensile strengths at various points during ISO 16630 HET. As on-line thickness measurement is not feasible with the present testing equipment, interrupted hole expansion testing was selected as a method for producing specimens from different points during the expansion process, followed by off-line thickness measurement by 3D scanning. The development of HER and thinning of the hole edge in different sheet directions were evaluated and compared with the machine instrumentation data collected during testing.

2 Methods and procedures

2.1 Research materials

The materials used in this study were industrially hot-rolled low-carbon (<0.06 wt.% C) steel strips with 3 mm nominal thickness. The steels were selected to have similar tensile strengths (835±10 MPa) in the material rolling direction while simultaneously having different microstructural constitutions. The used material coding refers to the dominant microstructure type of the material: CP having a complex-phase structure consisting of ferrite, bainite, and martensite, PF consisting of polygonal ferrite, and QF consisting of quasi-polygonal ferrite.

Tensile and hole expansion properties of the research materials of the present study have been investigated in previous works [7, 10]. The tensile properties in the rolling direction and material planar anisotropies are summarised in Table 1.

Table 1. Tensile properties tested in the material rolling direction and material planar anisotropies [10].

Material	R_m [MPa]	$R_{p0.2}$ [MPa]	A_g [%]	A_{80} [%]	Δr [-]
PF	757	845	9.1	16.4	-0.54
CP	751	846	5.8	11.5	-0.66
QF	751	828	9.1	17.4	-0.21

2.2 Interrupted hole expansion testing

110 x 100 mm pieces were cut from the steel sheets to obtain specimens for the hole expansion testing. The longer side was set along the material rolling direction. Two different preparation methods were applied to obtain 10 mm diameter holes to investigate effect of the edge condition on the performance: mechanical punching and wire electrical discharge machining (W-EDM). The hole punching was conducted using an Erichsen universal sheet metal testing machine applying 10 mm/min tool speed and 11.7% cutting clearance. For each material, 9 holes were punched, and 4 W-EDM specimens were prepared. Out of each combination, one hole was reserved for edge quality investigations.

The hole expansion tests (HET) were conducted according to ISO 16630 [2] set-up using an Erichsen universal sheet material testing machine equipped with a 60° tip angle conical expansion tool. The burr side of the specimen was set facing away from the expansion tool, and the tool was forced into the hole at 15 mm/min until a predetermined stop for the individual test was reached. A video feed was used to observe the expansion process.

The tests were interrupted at different expansion punch strokes to obtain specimens with various hole expansion ratios (HER). The different test interruption points for punched specimens were as follows, ordered by increasing expected punch stroke: (1) mid-point of an ISO 16630 HET, half of the expansion part of the punch stroke for the through-thickness crack appearance, (2) HER 20%, punch stroke to reach 20% HER estimated from video recording of an ISO 16630 HET, (3) prior to through-thickness crack appearance, stopping the test to a point where a potential crack for the failure has appeared, but not propagated through the thickness, (4) a standard ISO 16630 HET, stopping the test as a through-thickness crack is observed, and (5) an overshoot test, intentionally continuing the expansion for a short period after the through-thickness failure.

For the W-EDM specimens, only the prior to through-thickness crack appearance, standard ISO 16630, and overshoot tests were conducted. As the through-thickness fracture process is sudden in the W-EDM edges and interrupting the test during the crack propagation is difficult, for the W-EDM prior through-thickness crack appearance tests, the stopping point of the test was selected to be a point where significant thinning localisation in the edge is already observable.

Hole diameters were determined with caliper measurements before and after the testing from two perpendicular directions, and the limiting hole expansion ratios were calculated according to the standard [2]. Additionally, the machine instrumentation data (punch stroke, time, and drawing force) from both hole punching and expansion was collected for analysis.

Visual investigation was performed on the hole edge quality specimens and expanded HET specimens using a Dino-Lite Edge 3.0 handheld digital microscope.

2.3 3D scanning of expanded specimens

To investigate thinning of the hole edges, 3D scanning was performed on all expanded specimens excluding the overshoot tests. The process steps are visualised in Fig. 1. Prior to the scanning, the specimen surfaces were treated with an anti-glare spray and reference marker stickers were added. The 3D scans were performed using a GOM ATOS Triple Scan II optical surface scanner, equipped with two 5MP cameras with a resolution of 2448 x 2050. The specimens were scanned from both sides (Fig. 1a–b), and the data processing was carried out using the Zeiss GOM Inspect software. The scanned specimens were aligned to the coordinate system, after which three cross-sections were made: in 0° (rolling direction, RD), 45° (diagonal direction, DD), and 90° (transversal direction, TD) angle relative to the rolling direction (Fig. 1c–d).

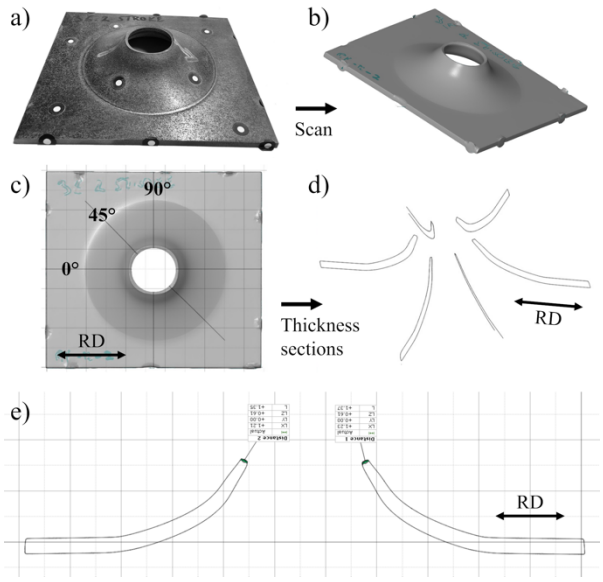

Fig. 1. Hole edge thinning measurement process: a) an expanded HET specimen (CP W-EDM prior t-t. crack), b) a 3D scan of the specimen, c) placement of the cross-section profile measurements around the hole, d) obtained thickness cross-section profiles in the three sheet directions, and e) determination of hole edge minimum thickness.

For each cross-section, the thinnest point from the expanded flange was determined (Fig. 1e). The result was then compared to the nominal thickness, allowing the maximum (plastic) thinning of the test specimens to be calculated.

3 Results and discussion

3.1 Hole punching

Example drawing force – punch stroke profiles for each material, and calculated mean maximum drawing force and punch strokes prior to fracture are presented in Fig. 2. Although the yield and tensile strengths were similar between the materials, differences in behaviour during punching were observed. In CP material, the maximum forces were lower, and a shorter punch stroke on average was required to fracture the material. QF material showed more variation in both results.

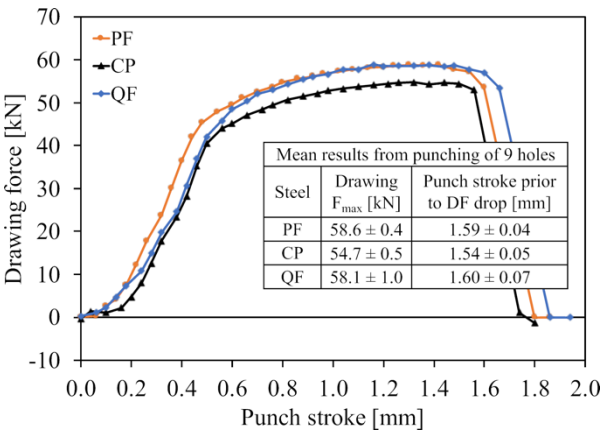

Mean results from punching of 9 holes

Steel	Drawing F_{max} [kN]	Punch stroke prior to DF drop [mm]
PF	58.6 ± 0.4	1.59 ± 0.04
CP	54.7 ± 0.5	1.54 ± 0.05
QF	58.1 ± 1.0	1.60 ± 0.07

Fig. 2. Example hole punching drawing force – punch stroke profiles and calculated mean results for punching of 9 holes. Standard deviations of the measurements are given.

Punched hole edge quality for each test material and an example of a W-EDM hole are presented in Fig. 3. CP had the best visual edge quality, fracture surface being smooth, whereas ferritic PF and QF materials displayed lamellar fracture behaviour and some secondary burnishing. The quality of the W-EDM edges was even, the hole surfaces being smoother compared to the rolling surfaces.

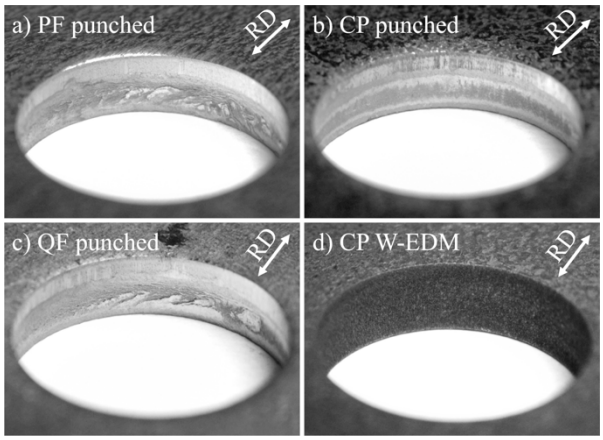

Fig. 3. Edge quality after preparation of a) PF punched, b) CP punched, c) QF punched, and d) CP W-EDM HET holes.

The quality of the punched edge had some correlation to the drawing force observed in the hole punching, as CP material with the best visual quality of the edge also displayed the lowest required maximum drawing force (CP 54.8 kN, QF 58.7 kN, and PF 59.4 kN, respectively, in Fig. 3). Similar trend was also observed with measured length of the burnish area (CP 0.72 mm, QF 0.86 mm, and PF 0.85 mm, respectively).

Secondary burnishing has been reported to be detrimental for stretch-flangeability [5], and its appearance might suggest that a slightly higher cutting clearance might be more optimal for quality of the sheared edge. However, in ferritic high-strength steels, increase in the cutting clearance can promote lamellar fracture behaviour [11], thus the optimisation of cutting can be challenging considering the changing tool clearances in production processes due to the tool wear.

3.2 Hole expansion

Hole expansion testing results of specimens with punched edges are summarised in Table 2 and results with W-EDM edges are summarised in Table 3. Expansion stroke is set to start at the point where the expansion tool reaches the specimen surface and drawing force starts to increase.

Considerably higher HER values were obtained for all test materials with W-EDM edge condition compared to the punched edge condition, which is expected due to the absence of high localised deformation and damage, such as microcracks and voids, introduced to the material edge during the punching process.

QF material showed superior HET performance with both punched and W-EDM edge conditions compared to the other two materials. In the present tests, HER did not correlate with quality of the sheared edge.

In CP material, which had the best visual quality of the edge, ISO test HER of the punched specimen was significantly higher compared to PF material, whereas with the W-EDM edge condition, difference between the two materials was decreased. It could be, that the improved edge quality is beneficial for punched condition HER of CP, but with the W-EDM edge in the absence of initial defects, other factors limit its performance. Differences in hardness between the different microstructures can promote local damage formation and limit the formability potential of the overall structure when the deformation is heavily localised during the expansion process. Additionally, CP had the highest planar anisotropy, and the absence of initial defects in the edge allows higher HER levels to be reached, simultaneously enabling the deformation to localise more severely in certain sheet directions.

Table 2. HET results of specimens with punched hole edge.

Test	Expansion stroke [mm]	Max. drawing force [kN]	HER [%]
PF – ISO mid-point	5.46	26.2	1
PF – prior t-t. crack	9.18	32.3	18
PF – HER 20%	10.08	33.4	19
PF – ISO 16630	10.78	35.7	22
PF – Overshoot	17.86	42.6	-
CP – ISO mid-point	7.86	31.2	8
CP – HER 20%	9.92	35.6	17
CP – prior t-t. crack	12.02	43.3	27
CP – ISO 16630	15.70	54.1	52
CP – Overshoot	21.00	57.2	-
QF – ISO mid-point	10.32	35.7	19
QF – HER 20%	10.94	37.8	22
QF – prior t-t. crack	15.44	56.9	51
QF – ISO 16630	20.60	72.7	83
QF – Overshoot	25.60	78.3	-

Table 3. HET results of specimens with W-EDM hole edge.

Test	Expansion stroke [mm]	Max. drawing force [kN]	HER [%]
PF – prior t-t. crack	29.62	124.4	130
PF – ISO 16630	31.34	123.9	141
PF – Overshoot	35.90	122.0	-
CP – prior t-t. crack	28.80	114.3	127
CP – ISO 16630	33.12	133.8	153
CP – Overshoot	34.46	125.2	-
QF – prior t-t. crack	38.78	176.3	190
QF – ISO 16630	40.92	190.8	204
QF – Overshoot	44.04	196.1	-

Although the HER 20% tests were successful in interrupting the HET close to the 20% HER value, there was some deviation between results, as the ratios were either slightly lower or higher than the indented 20%. Two contributing factors could be: (1) springback reducing the diameter of the hole after the tension is relieved after the retraction of the expansion tool, and (2) differences in local material properties and cracking behaviour during the testing between the HER 20% and the ISO specimen, of from which video recording the required stroke for the HER 20% test was estimated.

The ISO 16630 HET mid-point test results show that a part of the expansion stroke is spent on the initial flange formation prior the hole diameter can increase. This is especially seen with the result of the PF mid-point test, where a half of the expansion stroke leading to through-thickness crack is only resulting in a HER value of 1%.

Drawing force – expansion stroke curves from the different interrupted hole expansion tests are presented in Fig. 4a–c, combining both the punched and W-EDM edge tests.

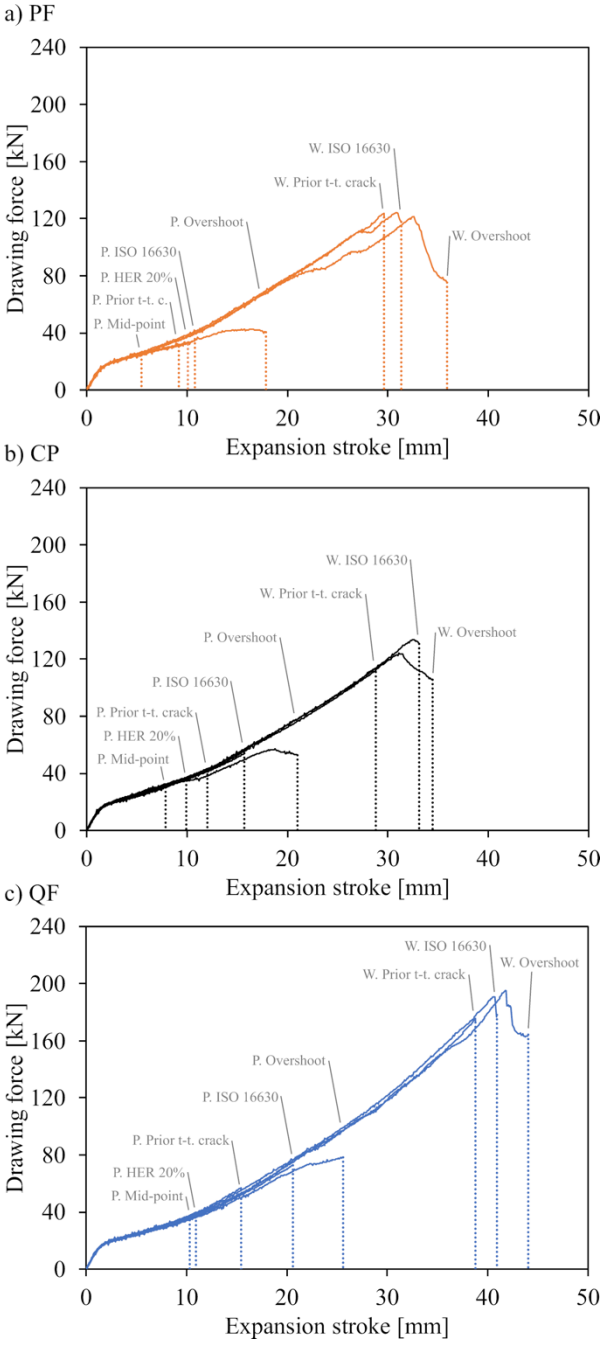

Fig. 4. Drawing force compared to expansion stroke during hole expansion testing of a) PF, b) CP, and c) QF specimens. P. = punched and W. = W-EDM specimens.

The drawing force – expansion stroke curves show similar behaviour between the materials in the beginning of the expansion, and more deviation appears near end of the tests. The curves of W-EDM specimens

seem to display more strain hardening compared to punched specimens. Some specimens show a short plateau in a part during the test prior to a continuation in increase of force, which could be a result of localisation of deformation during an individual test. The inherent scatter of the HET is also demonstrated in the CP material W-EDM tests, where a through-thickness failure occurred earlier in the overshoot test with a shorter expansion stroke compared to the ISO test. In general, appearance of a through-thickness crack was not clearly observed in drawing force – expansion stroke curves of punched specimens, whereas in W-EDM, a drop in the force was noticeable.

This effect is most likely related to the behaviour of the final fracture propagating through the material thickness. The failure in the W-EDM specimens occurs abruptly, and the continuing deformation is driven to propagate only a small number of fractures radially in the expanding flange. In the punched edges, a high number of small cracks is present significantly earlier during the test, and the competing cracks propagate relatively slowly through the material during the expansion. Additionally, the material in the flange away from the edge is not as deformed compared to a W-EDM specimen. These factors could explain why the drop in the force is not as abrupt with the punched specimens.

Correlations of measured maximum drawing force and hole expansion ratio to the expansion stroke at the interruption point of the test are presented in Fig. 5a and Fig. 5b, respectively.

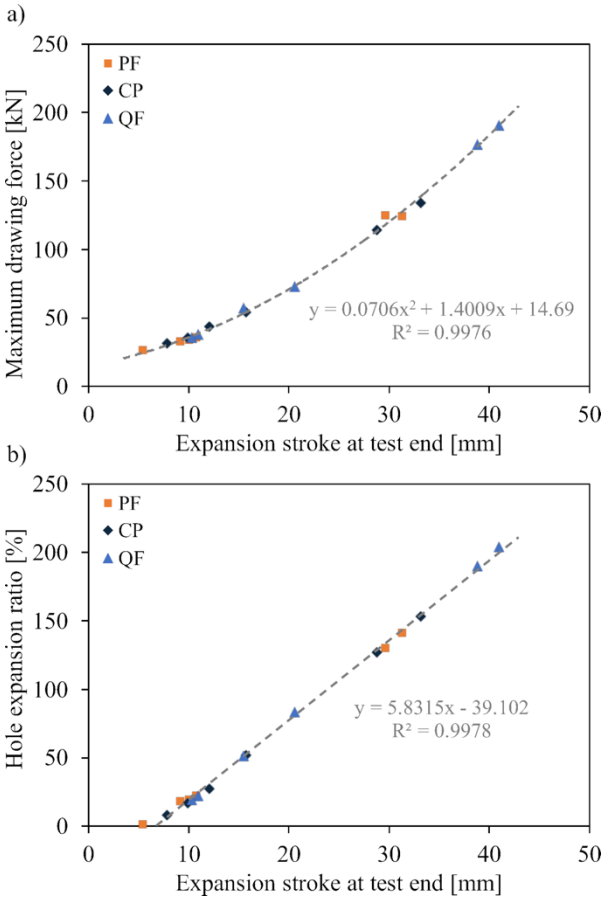

Fig. 5. Correlations of a) maximum drawing force during the testing and b) hole expansion ratio to expansion stroke at the test end. Overshoot tests are excluded.

Maximum drawing force increased non-linearly with the expansion stroke due to plastic deformation and increase in the size of the deformed flange. HER increased linearly after a certain stroke, which is to be expected based on the test set-up geometry. Some part of the measured stroke is spent for turning the edge upwards in the initial formation of the flange before HER can increase noticeably. Both Fig. 5a–b show good agreement between the different test materials due to the similar strength levels and initial sheet thickness.

3.3 Hole edge thinning

Maximum hole edge thinning measurement results are presented as comparison to HER in Fig. 6.

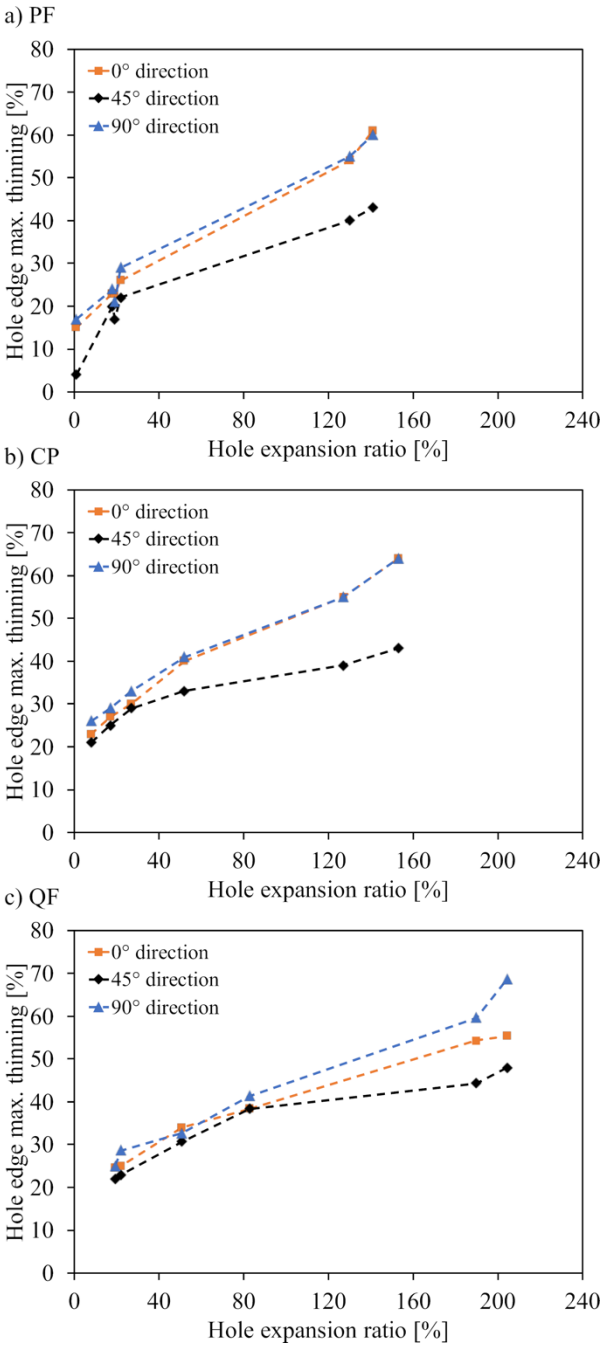

Fig. 6. Hole edge maximum thinning in the sheet rolling, diagonal, and transversal directions compared to hole expansion ratio in a) PF, b) CP, and c) QF specimens.

Localisation of thinning in the different sheet directions (RD, TD) is observable in the punched specimens even with the low HER values. The behaviour is more pronounced in the W-EDM specimens due to the higher amount of deformation. In QF, the thinning between the different directions is more uniform especially in punched specimens. In W-EDM specimens with higher HER levels, localisation will also increase in the QF material, however, the level still being lower compared to the PF and CP materials.

The results are in line with the material planar anisotropies. As the hole is expanded equally in all directions, higher anisotropy will allow deformation to concentrate in certain parts of the edge. The behaviour is also consistent with earlier investigation results of the same materials with punched edges, alternative HET tool set-ups, and DIC strain measurement [7], where local circumferential strain around the hole was observed to localise significantly in the material rolling and transversal directions prior to the failure.

In visual inspection of expanded HET specimens, localisation of edge thinning is clearly noticeable in W-EDM edges. Examples of through-thickness failure locations in punched and W-EDM specimens of PF material are presented in Fig. 7. Punched edges were generally filled with small propagating cracks, whereas the W-EDM edges have considerably fewer cracks. Localized deformation prior to the through-thickness crack formation can be seen in Fig. 7b.

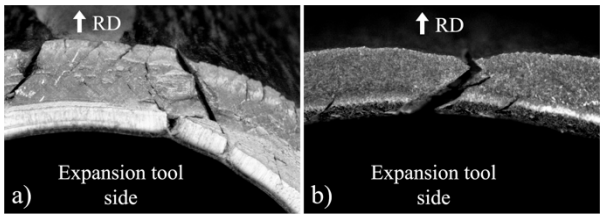

Fig. 7. Examples of through-thickness failures in expanded a) PF punched and b) PF W-EDM ISO 16630 specimens.

In future research, more detailed investigations will be conducted on the interrupted hole expansion test specimens to further examine fracture behaviour and development of damage near the expanding edge.

4 Conclusions

The results led to the following conclusions:

- Hole punching of CP required a lesser maximum force and a shorter punch stroke compared to the ferritic steels, which was also reflected in improved quality of the edge.
- However, HER did not correlate with the visual quality of the punched edge, suggesting that HET performance cannot always be predicted based on the overall sheared edge quality.
- HER correlated linearly with expansion punch stroke after initial flange formation for all tested materials due to the geometry of the test set-up.
- Appearance of a through-thickness crack was not clearly observed in drawing force – expansion stroke curves of specimens with a punched edge. In W-EDM specimens, a drop in the force was observed after through-thickness crack formation, indicating a more abrupt fracture process.
- With the 3D thickness measurements, plastic thinning of the edge was observed to localise in the sheet rolling and transversal directions. The effect was more pronounced in the W-EDM specimens, but also noticeable in the punched specimens.
- Although localisation of thinning was also present in QF, which had superior performance with both punched and W-EDM edge conditions, the behaviour was less pronounced compared to the other investigated steels, resulting from the lesser degree of planar anisotropy.

Acknowledgements

The authors are grateful to the funding for the research from the projects FOSSA II (Fossil-Free Steel Applications: Phase 2, grant number 5562/31/2023) by Business Finland and FormFuture (Potential of Advanced Forming Technologies in the Future Carbon Neutral Engineering Workshops, code A80637) by The Regional Council of Lapland.

References

1. B.S. Levy, C.J. Van Tyne, J. Mater. Eng. Perform., **21**, 1205 (2012)
2. International Organization for Standardization, ISO 16630:2017 Metallic materials – Sheet and strip – Hole expanding test (2017)
3. E. Atzema, M. Borsutzki, M. Braun, S. Brockmann, M. Bülter, B. Carlsson, P. Larour, A. Richter, Proc. Int. Conf.: N. Dev. Sheet Met. Form., 171 (2012)
4. N. Pathak, C. Butcher, M. Worswick, J. Mater. Eng. Perform., **25**, 4919 (2016)
5. P. Larour, J. Hinterdorfer, L. Wagner, J. Freudenthaler, A. Grünsteidl, M. Kerschbaum, IOP Conf. Ser.: Mater. Sci. Eng., **1238**, 012041 (2022)
6. I.A. Denks, M. Schneider, S. Westhäuser, C. Lesch, Steel Res. Int., **90**, 1 (2019)
7. P. Plosila, V. Kesti, A. Kaijalainen, R. Vierelä, P. Rautio, J. Kömi, IOP Conf. Ser.: Mater. Sci. Eng., **1284**, 012022 (2023)
8. M. Schneider, A. Geffert, I. Peshekhodov, A. Bouguecha, B.A. Behrens, Mat.-wiss. u. Werkstofftech., **46**, 1196 (2015)
9. V. Kesti, M. Folmerz, R. Vierelä, P. Rautio, R. Ruoppa, P. Plosila, A. Kaijalainen, IOP Conf. Ser.: Mater. Sci. Eng., **1238**, 012035 (2022)
10. P. Plosila, V. Kesti, J. Hannula, J. Kömi, A. Kaijalainen, Mater. Today Commun., **40**, 109521 (2024)
11. A. Kaijalainen, V. Kesti, R. Vierelä, M. Ylitolva, D. Porter, J. Kömi, J. Phys.: Conf. Ser. **896**, 012103 (2017)